Pharm Res (2015) 32:1764–1778
DOI 10.1007/s11095-014-1574-1

RESEARCH PAPER

Model-Based Evaluation of the Impact of Formulation and Food Intake on the Complex Oral Absorption of Mavoglurant in Healthy Subjects

Thierry Wendling • Kayode Ogungbenro • Etienne Pigeolet • Swati Dumitras • Ralph Woessner • Leon Aarons

Received: 21 August 2014 / Accepted: 10 November 2014 / Published online: 26 November 2014

ABSTRACT

Purpose To compare the pharmacokinetics of intravenous (IV), oral immediate-release (IR) and oral modified-release (MR) formulations of mavoglurant in healthy subjects, and to assess the food effect on the MR formulation's input characteristics.

Methods Plasma concentration-time data from two clinical studies in healthy volunteers were pooled and analysed using NONMEM®. Drug entry into the systemic circulation was modelled using a sum of inverse Gaussian (IG) functions as an input rate function, which was estimated specifically for each formulation and food state.

Results Mavoglurant pharmacokinetics was best described by a two-compartment model with a sum of either two or three IG functions as input function. The mean absolute bioavailability from the MR formulation (0.387) was less than from the IR formulation (0.436). The MR formulation pharmacokinetics were significantly impacted by food: bioavailability was higher (0.508) and the input process was shorter (complete in approximately 36 *versus* 12 h for the fasted and fed states, respectively).

Conclusions Modelling and simulation of mavoglurant pharmacokinetics indicate that the MR formulation might provide a slightly lower steady-state concentration range with lower peaks (possibly better drug tolerance) than the IR formulation, and that the MR formulation's input properties strongly depend on the food conditions at drug administration.

KEY WORDS dose superimposition · food effect · input rate function · mavoglurant population pharmacokinetics · modified-release formulation

ABBREVIATIONS

BQL	Below the quantification limit
BW	Actual bodyweight
CL	Plasma clearance
IG	Inverse Gaussian
IMPMAP	Monte Carlo importance sampling method assisted by mode a posteriori with interaction
IR	Immediate-release
ISV	Intersubject variability
IV	Intravenous
mGluR5	Metabotropic glutamate receptor 5
MR	Modified-release
OFV	Objective function minimum value
Q	Inter-compartmental clearance
Vc	Volume of distribution of the central compartment
Vp	Volume of distribution of the peripheral compartment

INTRODUCTION

Mavoglurant is a structurally novel, subtype-selective, non-competitive antagonist at the metabotropic glutamate

Electronic supplementary material The online version of this article (doi:10.1007/s11095-014-1574-1) contains supplementary material, which is available to authorized users.

T. Wendling • K. Ogungbenro • L. Aarons (✉)
Manchester Pharmacy School, The University of Manchester
Manchester, UK
e-mail: leon.aarons@manchester.ac.uk

T. Wendling • S. Dumitras • R. Woessner
Drug Metabolism and Pharmacokinetics, Novartis Institutes for Biomedical Research, Basel, Switzerland

E. Pigeolet
Pharmacometrics, Novartis Pharma AG, Basel, Switzerland

receptor 5 (mGluR5). It is currently under clinical development (Novartis Pharma AG, Basel, Switzerland) for the treatment of fragile X syndrome, which is the most common hereditary form of mental retardation (1) and the most common single genetic cause of autism (2–5) in humans. The typical phenotype includes intellectual disability, developmental delays and behavioural disorders, and is usually diagnosed in young children (6). By blocking the glutamatergic signalling through mGluR5, mavoglurant is thought to have the potential to rescue the disease state (7–10). A recent study in adult males showed that behavioural symptoms of fragile X syndrome can be improved by mavoglurant treatment (11), but efficacy needs to be confirmed in lager clinical studies. Also, a study of the effect of mavoglurant on obsessive-compulsive disorder in patients resistant to selective serotonin reuptake inhibitor therapy, has been conducted (ClinicalTrials.gov identifiers NCT01813019). A good understanding of mavoglurant pharmacokinetics in healthy subjects is required to determine its optimal conditions of use in the target populations. In this view, it is important to select a formulation that produces steady-state plasma concentration resulting in a desirable therapeutic effect while providing a safe and convenient dosing for patients.

Mavoglurant is intended to be administered by the oral route. The pharmacokinetics of mavoglurant after oral administration of a single 200 mg ^{14}C-radiolabeled dose in four healthy males, was described recently: the extent of absorption was ≥50% of the total dose; it is a neutral and very lipophilic compound (logP of 4.7) and was therefore extensively distributed to organs and tissues (the mean apparent terminal volume of distribution was estimated to be 38.7 l/kg); the blood-to-plasma concentration ratio and unbound fraction to plasma proteins were estimated to 0.61 and 0.028, respectively; its elimination occurred primarily by oxidative metabolism leading to the formation of seven metabolites which accounted for 60% of the systemic exposure to the total radioactivity over 72 h; the estimate of mean apparent plasma clearance was 2.07 l/h/kg; based on the metabolites observed in human excreta and prior *in vitro* metabolism results, the major biotransformation pathway was thought to involve cytochromes P450 2Cs, 3A4, 1A1 and 2D6 and accounted for 56% of total metabolism (12). An immediate-release (IR) hard gelatine capsule formulation that requires a twice-daily dosing regimen was first used in human clinical studies. Since in these studies, the majority of adverse events attributed to mavoglurant treatment (dizziness, dyskinesia, hallucination and fatigue) were assumed to be peak plasma concentrations related (13,14), a modified-release (MR) matrix tablet was developed in order to reduce peak plasma concentrations without substantial change in the plasma exposure to mavoglurant. The pharmacokinetics of the IR and MR formulations were compared in a Phase I study in healthy volunteers in order to guide formulation selection for further clinical development. Since mavoglurant is poorly soluble in aqueous solution (pH independent solubility of 0.025 mg/ml) but well absorbed *in vivo* (highly permeable) (12), it is considered as a Class II compound in the Biopharmaceutics Classification System. Furthermore, since it is extensively metabolised, it is assumed to be also a Class II compound in the Biopharmaceutics Drug Disposition Classification System (15). Therefore, an increase in the extent of bioavailability was suspected for concomitant administration with a high fat meal, and was investigated for the MR formulation.

The goals of this analysis were to develop and evaluate a nonlinear mixed-effects model to (i) describe mavoglurant disposition in a healthy population and identify any contributing demographic covariate factors, (ii) characterise and compare mavoglurant input rate and bioavailability from the IR and MR formulations, (iii) quantify the effect of a high fat meal on the bioavailability and input rate of the MR dosage form, and (iv) predict the impact of mavoglurant release-rate and of concomitant food intake on the concentration range provided by a twice-daily repeated administration. To overcome potential identifiability issues when mathematically characterising the input kinetics of a prolonged-release formulation, it is necessary to inform drug disposition with data provided by the intravenous (IV) route. Therefore, pharmacokinetic data following IV administration of mavoglurant in healthy volunteers were extracted and included in the analysis. Following oral administration, mavoglurant plasma concentration-time profiles appeared to be complex and highly variable across the studied subjects. For instance, an erratic multiple-peak phenomenon was observed in individual profiles after administration of both the IR and MR formulations under fasted conditions. Since plasma concentrations following IV administration clearly revealed two exponential phases of drug disposition and did not exhibit multiple peaks, it was assumed that the complexity of the pharmacokinetics arose from the absorption process. Complex input profiles are difficult to characterise using conventional absorption models that assume a first-order or zero-order input rate for a fixed period. For orally administered drugs, more mechanistic models that incorporate, to a certain extent, physiological factors involved in the absorption process are difficult to implement when the underlying mechanism is unknown (16). Therefore, a flexible empirical model describing the erratic input transit time of orally administered mavoglurant was sought in this analysis.

DATA AND METHODS

Clinical Data

Frequently sampled pharmacokinetic data from two clinical studies in healthy volunteers were pooled to form the data set

used in the analysis (Table I). The majority of subjects were young (median age of 28 years) Caucasian (90.2%) males (72.0%) with a median weight of 80.3 kg.

Study A2121 was conducted to quantify the effect of single IV doses of mavoglurant on baseline- and placebo-corrected QTc intervals in healthy subjects, as well as to characterise the pharmacokinetics of mavoglurant following a 10-min IV infusion. The first part of the study (Part A) was a single-ascending dose phase during which three parallel groups of 12 subjects received either a dose of 25, 37.5 or 50 mg. In the second part (Part B), 84 subjects received two doses of 25 and 50 mg in a randomized crossover design. Plasma concentration-time data from 120 subjects in total were available.

The objective of Study A2167 was to compare the pharmacokinetic properties of three different oral prolonged-release formulations of mavoglurant after a single 100-mg dose in healthy subjects, with reference to a 50-mg single dose in two IR capsules (25 mg/capsule), and to evaluate the effect of a high-fat (≈50% of the meal's total calories) and high-calorie (≈800–1000 calories) breakfast on the pharmacokinetics of the prolonged-release forms. Medication was thus given either under fasted conditions or within 5 min of completion of a high fat meal. 44 young Caucasian male volunteers were to receive a total of five single doses of mavoglurant out of the seven treatments tested. The three prolonged-release forms differed by the time window within which the drug was intended to be released in the gastrointestinal tract (6, 7 and 8 h). Since the formulation developed to release mavoglurant over 8 h (denoted MR in the present work) was selected for further clinical development, data for the other prolonged-release formulations were excluded from this analysis. Hence, three treatments were retained for the herein model-based analysis: a 50-mg dose in IR capsules under fasted conditions (IR-fasted), a 100-mg dose in the MR tablet under fasted conditions (MR-fasted) and a 100-mg dose in the MR tablet under fed conditions (MR-fed). A total of 16 subjects discontinued the study due to adverse events, or withdrew consent. While all subjects completed the IR-fasted period, only 29 subjects were administered a dose as per the MR-fasted treatment and 28 subjects received the MR-fed treatment.

Additional pharmacokinetic data from a study of the effect of three different meal compositions and three different timing of food intake on the pharmacokinetics of mavoglurant following a single oral administration of the 100-mg MR tablet

Table I Subjects Demographics and Designs of the Clinical Studies of Mavoglurant Pharmacokinetics in the Healthy Subjects Included in the Population Analysis

Characteristic	Analysed data set		
	Study A2121	Study A2167	Combined
Design	Randomized, partially-blinded, active-comparator controlled, crossover, two sequential parts: pilot single-ascending dose phase (Part A) and core thorough QTc phase (Part B)	Randomized, open-label, cross-over, three periods, single dose	
No. of subjects	Part A: 36 Part B: 84	44	164
Age (years)	31 (18–50)	24 (19–45)	28 (18–50)
Gender (%)	Male = 86.7	Male = 100	Male = 90.2
	Female = 13.3	Female = 0	Female = 9.8
Race (%)	Caucasian (61.7), Black (30), Native American (1.7) and Other (6.7)	Caucasian (100)	Caucasian (72.0), Black (22.0), Native American (1.2) and Other (4.9)
Weight (kg)	82.8 (56.6–115.3)	76.7 (61.1–97.0)	80.3 (56.6–115.3)
Body mass index (kg/m^2)	26.5 (18.7–32.2)	23.8 (20.5–29.0)	25.7 (18.7–32.2)
Route / formulation	IV / 10 min infusion	Oral / IR capsule and MR tablet	
Dose (mg)	Part A: 25, 37.5 or 50	50 (IR) and 100 (MR)	
	Part B (crossover): 25 and 50		
Food conditions	Fasted	Fasted (IR and MR) / fed (MR)	
PK sampling schedule	Part A: predose and at 0.25, 0.33, 0.5, 0.67, 1, 2, 3, 4, 6, 8, 12, 24, 36 and 48 h postdose Part B: predose and at 0.33, 0.5, 0.67, 1, 2, 3, 4, 6, 8, 12 and 24 h postdose	Predose and at 0.5, 1, 1.5, 2, 3, 4, 6, 8, 10, 14, 24, 36, 48 and 72 h postdose	
Typical no. of samples/subject	Part A: 14 Part B: 24	29	3483[a]

Continuous variables are given as median (range) and were reported for all subjects

[a] Total number of samples

in healthy subjects (Study A2171), were used for cross-validation of the final model rather than in the analysis (Table II). Thirty-eight healthy volunteers were administered a total of five single doses of mavoglurant: one dose under fasted conditions and four doses under fed conditions. Since the meal compositions were substantially different from the composition of the high fat breakfast assessed in Study A2167, data from the fed periods were excluded for external validation of mavoglurant pharmacokinetic model.

All studies were conducted according to the ethical principles of the Declaration of Helsinki and all protocols were approved by the Institutional Review Board for the study centers. The study participants were males and non-pregnant females over the age of 18 years and all provided full written informed consent prior to inclusion in the studies.

In all studies, mavoglurant concentrations in plasma were determined by a validated liquid chromatography-tandem mass spectrometry method (17). The lower limit of quantification was 2 ng/ml. Concentrations below this limit were labeled as zero.

Pharmacokinetic Data Analysis and Modelling Methods

A total of 3483 concentration-time observations of 164 healthy subjects were available for the model-based analysis. Since the data were of population type, a nonlinear mixed-effects modelling approach was applied using the software NONMEM® (version VII, level 2.0) (18). NONMEM runs were conducted using the software tool Pearl-speaks-NONMEM 3.5.3 (19). The first-order conditional estimation method with interaction was first used for parameter estimation during model building. Since numerical issues were experienced with this method, we resorted to a Monte Carlo importance sampling method assisted by mode a posteriori with interaction (IMPMAP) to estimate the standard value of the pharmacokinetic parameters in the population, random intersubject variability (ISV) and random interoccasion variability in these parameters, and residual variability between model predictions and observed plasma concentrations. The random residual variability may arise from unexplained within-subject variability, model misspecification and experimental error. Correlations between variability components were tested. Using the IMPMAP estimation method, the number of iterations (NITER option in NONMEM) and the number of random samples per individual (ISAMPLE) were set to 3000 and 1000, respectively. Convergence was tested on the objective function, fixed-effects, random-effects (diagonal elements of the variance-covariance matrix only, *i.e.* option CTYPE=2) and the residual error. To evaluate the convergence, a linear regression test was performed on the 10 (CITER=10) most recent, consecutive (CINTERVAL=1) iterations with an alpha error rate of 5% (CALPHA=0.05). Observations below the lower limit of quantification were discarded during the analysis. The statistical package R (version 2.15.1) (20) was used for exploratory data analysis and to produce descriptive statistics of demographics prior to the population analysis; for graphical assessment of NONMEM outputs during model building.

Table II Subjects Demographics and Design of the Clinical Study of Mavoglurant Pharmacokinetics in the Healthy Subjects Included for the External Validation of the Final Model

Characteristic	Validation data set Study A2171
Design	Randomized, open-label, crossover, single dose
No. of subjects	38
Age (years)	26 (19–44)
Gender (%)	Male = 80.5
	Female = 10.5
Race (% of total no. of subjects)	Caucasian (55.3) and Black (44.7)
Weight (kg)	77.7 (61.6–105.6)
Body mass index (kg/m^2)	27.0 (21.2–29.8)
Route / formulation	Oral / MR tablet
Dose (mg)	100
Food conditions	Fasted
PK sampling schedule	Predose and at 1, 2, 3, 4, 5, 6, 8, 10, 14, 24, 36 and 48 h postdose
Typical no. of samples/subject	12

Continuous variables are given as median (range) and were reported for all subjects

Model selection was achieved by use of the objective function minimum value (OFV) as goodness-of-fit statistic, as well as by examination of the NONMEM-provided asymptotic standard errors on each parameter estimate and goodness-of-fit plots. The OFV is minus twice the logarithm of the maximum likelihood of the model. Differences between objective functions of two fits of hierarchical models to the same data are approximately chi-squared distributed with degrees of freedom equal to the difference in the number of parameters between models. A significance level of 0.05 was considered for the likelihood ratio test during model building, meaning that, a drop of >3.84 in the objective function after addition of a single model parameter, was deemed a statistically significant improvement of the model.

In the preliminary stage of model building, one- and two-compartment disposition models, with linear and non-linear elimination from the central compartment, were fitted to IV data alone although graphical inspection of the concentration-time curves revealed a clear bi-exponential decrease in plasma concentrations and no signs of nonlinearity with the dose. Thereafter, concentration-time data provided by both the

IV and oral routes were modelled simultaneously in order to characterise the input and disposition kinetics during the same analysis. Conventional absorption models, as well as a transit compartment model (21) and models assuming parallel or sequential zero- and first-order absorption rates (22), were initially used to describe drug input after oral administration of mavoglurant. The absorption component of the model was subsequently modified as described in the next paragraph. ISV was assessed on all structural model parameters as exponential variance and was defined as being normally distributed with mean zero and variance ω^2. Interoccasion variability was assessed following the method proposed by Karlsson and Sheiner (23). The residual error was modelled as additive to the logarithmically-transformed observed concentrations and was defined as being normally distributed with mean zero and a homogenous variance σ^2. Another error model for logarithmically-transformed observations, described by Beal, was assessed (24).

Because of the irregular complexity of individual concentration-time profiles following oral administration of mavoglurant, drug entry into the systemic circulation was eventually modelled using a flexible input rate function. The method proposed by Csajka *et al.*, which uses a weighted sum of n inverse Gaussian (IG) density functions as an analytical solution of the input transit time model, was considered (25). The input function was hence expressed as follows:

$$I(t) = F \cdot D \cdot \sum_{j=1}^{n} f_j \cdot IG_j(t) \tag{1}$$

where F is the bioavailability from the drug formulation, D is the administered dose (in mg), f_j is a weight parameter attached to the j^{th} IG density function, $IG_j(t)$, such that $\sum_{j=1}^{n} f_j = 1$. $IG_j(t)$ is given by the following equation:

$$IG_j(t) = \sqrt{\frac{MIT_j}{2\pi \cdot CV_j{}^2 \cdot t^3}} \times \exp\left[-\frac{(t - MIT_j)^2}{2CV_j{}^2 \cdot MIT_j \cdot t}\right] \tag{2}$$

In Eq. (2), t is the time after dose administration (in h), MIT_j is the mean of the j^{th} IG distribution, and CV_j is the coefficient of variation of MIT_j (normalised variance of the j^{th} IG distribution). MIT_j was calculated from an estimate of the mode of the j^{th} density, $tmax_j$, as follows (26):

$$MIT_j = tmax_j \Big/ \left[\sqrt{1 + \frac{9}{4} CV_j{}^4} - \frac{3}{2} CV_j{}^2\right] \tag{3}$$

$tmax_j$ is in fact the time at which the j^{th} input rate reaches its maximum. Estimating $tmax_j$ rather than MIT_j allows the information on each of the n IG functions to be reduced to a single measure, as $tmax_j$ depends on both MIT_j and CV_j (26). The model was expressed using the following ordinary differential equations (using NONMEM subroutine ADVAN13):

$$\frac{dA_1}{dt} = I(t) - A_1 \cdot (k_{10} + k_{12}) + A_2 \cdot k_{21} \tag{4}$$

$$\frac{dA_2}{dt} = A_1 \cdot k_{12} - A_2 \cdot k_{21} \tag{5}$$

Where $I(t)$ is a single IG function or a sum of two or three IG functions (Eqs. (1) and (2)); A_1 and A_2 are the amounts of drug (in mg) in the central and peripheral compartments, respectively; k_{10} (h^{-1}) is the first-order rate constant accounting for the elimination of drug from the body; and k_{12} and k_{21} (h^{-1}) are the first-order rate constants associated with drug transfer from the central to the peripheral compartment and *vice versa*, respectively.

A "saturated" stochastic model, in which random effects were assigned to all parameters of each IG function, was used in the analysis (25). However, to avoid potential random-effect identifiability issues, the same variances ω^2_{tmax} and ω^2_{CV} were estimated for all $tmax_j$ and CV_j (for $j = 1,..,n$) of the n IG functions, respectively. This can be done by using the "SAME" option when defining the variance-covariance matrix in NONMEM (see NONMEM guide VIII). Considering the example of a sum of two IG functions, this means that the random effects on $tmax_1$ and $tmax_2$, as well as on CV_1 and CV_2, can be different at the individual levels since they are sampled from different distributions that have the same variance. To avoid flip-flop between the IG densities and allow a natural ordering of the n input rates, the constraint $tmax_{j,i} \geq tmax_{j-1,i}$ was imposed as follows (25):

$$tmax_{j,i} = tmax_{j-1,i} + \theta_{tmax_j} \cdot e^{\eta_{tmax_{j,i}}} \tag{6}$$

for $j = 2,..,n$, and where θ_{tmax_j} is the standard value of $tmax_j$ in the population and $\eta_{tmax_{j,i}}$ is the ISV in $tmax_j$ for the i^{th} individual. At the individual levels, the constraint $0 \leq F_i \leq 1$ was imposed by defining the parameter as logit-normally distributed in the population, using the following equation:

$$F_i = \frac{e^{[\theta_F + \eta_{F_i}]}}{1 + e^{[\theta_F + \eta_{F_i}]}} \tag{7}$$

where θ_F is the logit-transformation of the standard value of F in the population and η_{F_i} is the ISV in the logit-transformed F for the i^{th} individual. For a sum of two IG functions ($n = 2$), the constraint $\sum_{j=1}^{n} f_{j,i} = 1$ was simply imposed by defining the first weight parameter f_1 as logit-normally distributed such that $0 \leq f_{1,i} \leq 1$ for individual i, and deriving the second weight parameter as $f_{2,i} = 1 - f_{1,i}$. However, for a sum of more than two IG functions ($n > 2$), constraining the joint distribution of the f_j parameters such that $\sum_{j=1}^{n} f_{j,i} = 1$

while ensuring that $0 \leq f_{j,i} \leq 1$ for $j=1,..,n$, was performed by assigning a multivariate logistic-normal distribution to the individual f_j parameters. The details about the implementation and application of the logistic-normal distribution in nonlinear mixed-effects models were provided by Nikolaos Tsamandouras (personal communication, June 20, 2014). In the present work, since f_j can be interpreted as the fraction of bioavailable-dose reaching the systemic circulation as per the j^{th} IG density, imposing the constraint $0 \leq f_{j,i} \leq 1$ allows consistency with physiology.

From the graphical assessment of the raw data, it was evident that the absorption process exhibited different patterns depending on the formulation and food state at drug administration. To increase the flexibility of the absorption model, the input function was defined specifically for each oral formulation and food status, *i.e.* specifically for each treatment of Study A2167. Three different input functions were thus optimised rather than testing the formulation and food-status variables as categorical covariates for the input parameters. Both fixed- and random-effects were allowed to be different across the three input functions. To ease the determination of the number of IG functions that would best describe mavoglurant input under each condition (IR-fasted, MR-fasted and MR-fed), each subset of Study A2167 data was first analysed separately with IV data. Furthermore, given the complexity of the pharmacokinetic model, the program Popdes 4.0 (27) was used to evaluate the design of Study A2121 and Study A2167, and predict the standard errors of the parameter estimates obtained with the "saturated" stochastic model. Once the input functions were deemed adequate, model building was pursued by analysing the pooled data set described in Table I.

Relationship between the demographic variables age and actual bodyweight (BW), and the disposition parameters were tested. Lean bodyweight, fat bodyweight (expected amount of fat for a normal-weight individual) and predicted normal weight (descriptor of weight for overweight and obese individuals) were tested as other surrogates for subjects' weight (28). Since most subjects were Caucasian (72.0%) males (90.2%), the race and gender variables were not tested as covariates in the model. Potential parameter-covariate relationships were initially identified by graphical assessment of the empirical Bayes estimates of the parameters plotted against individual covariate values, given that the shrinkage magnitude in the structural parameters was not too high (≤30%) (29). The selected covariates were then tested in the model by stepwise addition using an OFV drop of >10.83 (chi-squared value for $p \leq 0.001$ and a single degree of freedom) as inclusion criteria, followed by stepwise deletion using an OFV increase of >12.12 (chi-squared value for $p \leq 0.0005$ and a single degree of freedom) as criteria for retaining the covariate in the model.

Pearl-speaks-NONMEM was used to run a nonparametric bootstrap of 200 samples in order to estimate the standard errors on the model parameters. Since only data from Study A2167 were informative for the estimation of absorption parameters, resampling from the original pooled dataset was stratified by clinical study. Thereby, the proportion of subjects from Study A2121 (73%) and Study A2167 (27%) remained identical in the bootstrap datasets. All runs were included when calculating the bootstrap results.

Validation of the Pharmacokinetic Model

The software R was used to perform a visual predictive check that provides an assessment of the final model's ability to describe the data and its suitability for simulation. The visual predictive check was stratified by study, dose (for Study A2121) and treatment (for Study A2167). For each stratum, 1000 new datasets with identical design to the original data subset were generated using the final model. The concentrations in each original data subset were binned to create concentration intervals corresponding to the nominal observation times. Within each bin, the median concentration, along with the 5th and 95th percentiles, were calculated from the observed subset of data. For each stratum, the 5th, 50th and 95th percentiles were computed for each of the 1000 simulation runs. Thereby, a 95% confidence interval around the median could be calculated for each predicted percentile. To evaluate the predictive performance of the model with respect to both uncensored and left-censored data, the visual predictive check was shown for each stratum in two panels: the top panel compared the median of the predicted concentrations as well as a 90% prediction interval, with the observations; the bottom panels showed the fraction of plasma samples below the quantification limit (BQL) along with a simulation-based 95% confidence interval around the median of the predicted BQL data (30).

An external validation was also performed by comparison of the model with an independent data set. Using Study A2171 data, only the performance of the MR-fasted input function together with the disposition model could be evaluated. Parameter estimates of the final MR-fasted model were used to simulate 1000 new datasets with identical design to Study A2171 (Table II). A visual predictive check was then performed similarly to the internal validation of the model described in the previous paragraph.

Simulations

For each formulation and food state, the standard time course of mavoglurant input rate following a single 100-mg dose was simulated in R using Eq. (1) and the final population mean

estimates of the input parameters. Similarly, the typical time course of the bioavailability $F_A(t)$, was simulated using the following equation:

$$F_A(t) = F \cdot \sum_{j=1}^{n} f_j \cdot F_{Aj}(t) \quad (8)$$

with $F_A(\infty)=F$ and where $F_{Aj}(t)$ is the j^{th} cumulative IG distribution function of time, provided by the R function *pinvgauss()*.

NONMEM was used to simulate 1000 individual plasma concentration-time profiles following a twice-daily repeated administration (100 mg/dose) of IR capsules under fasted conditions and of MR tablets under both fasted and fed conditions, over eight dosing intervals to ensure attainment of steady-state. For each of the three treatments, the median concentration-time curve was plotted along with a 95% prediction interval. To eliminate the assumption that a dose has been completely absorbed prior to the next dosing event, dose superposition was implemented in NONMEM by adapting the method proposed by Shen *et al.* to the herein input function (31). This method allows the analytical solution of the input model (Eq. (1)) to be used for a repeated dose regimen. Three user-defined functions (FUNCA, FUNCC and FUNCB), *i.e.* one for each of the *n* weighted IG functions, were defined in a single FORTRAN code (see Appendix 1 in the Supplementary Material online). The user-supplied FORTRAN subroutine was then called in a NM-TRAN code using the "OTHER" option in NONMEM (see Appendix 2 in the Supplementary Material online). When using the first-order or first-order conditional estimation methods, NONMEM requires the first partial derivatives of the functions with respect to the variables associated with random effects to compute the objective function (see NONMEM guide VIII). Although the partial derivatives were not essential for the present simulations, they were provided in the FORTRAN code for further use of the subroutine. Specification of the partial derivatives has been verified using the MR-fasted final model, according to the method described by Shen *et al.* (31) (details in the Supplementary Material online).

RESULTS

Population analysis of the pooled intravenously and orally administered mavoglurant concentration-time data allowed the kinetics of drug input rate and disposition to be described simultaneously. Mavoglurant disposition was best described using a two-compartment model with linear elimination from the central compartment. Using conventional absorption models or the transit compartment model to describe the arbitrarily complex absorption profiles (*e.g.* double-peak phenomenon), clearly led to model misspecification. In contrast, using a weighted sum of two or three IG functions as an input rate function offered sufficient flexibility to allow a reasonable fitting of the pharmacokinetic model to all data following oral administration of mavoglurant. The use of a single IG function as an input function provided a reasonable description of the concentration-time profiles provided by the IR-fasted treatment, but did not capture the double-peak phenomenon observed in approximately 20% of the individual profiles. The addition of a second IG function substantially increased the flexibility of the input function thereby providing a much better fitting to data from all subjects. Since after the MR-fasted dose, the majority of subjects exhibited a more or less smooth re-increase in their plasma concentrations starting within 8–14 h of administration, a single IG function was not tested to model the drug's input rate. A sum of two IG functions did not capture the late re-increase in the concentrations. The addition of a third term allowed an acceptable description of the complex concentration-time profiles. The double-peak phenomenon was not observed when the MR tablet was administered within 5 min of completion of a high fat breakfast. However, most of individuals' concentration-time profile were characterised by a slow initial increase in the plasma concentrations within 2–6 h of administration, followed by a rapid rise toward the maximum. A sum of two IG functions as an input function provided an adequate description of this pattern.

The model was parameterised in terms of plasma clearance (CL), volume of distribution of the central compartment (Vc), inter-compartmental clearance (Q) and volume of distribution of the peripheral compartment (Vp) for the disposition parameters; in terms of F, f_1, f_2, $t\max_1$, $t\max_2$, $t\max_3$, CV_1, CV_2 and CV_3 for the parameters of each input function (Eqs. (1–3)). The final model is illustrated in Fig. 1.

Prediction of the standard errors of the parameter estimates revealed that the study designs did not allow ISV in all parameters to be estimated accurately. Hence, the variances of the random-effects on CV_1 and CV_2 of the IR-fasted input function, and on f_1 of the MR-fed input function, were fixed to a small value (0.0001 to represent a 1% coefficient of variation for a log-normally distributed parameter) rather than being estimated. Since the model included many input parameters that didn't have any clear biological meanings, correlations were tested only between the disposition parameters. Strong correlations between CL and Vc (0.652) and between Q and Vp (0.845) were estimated. Nevertheless, for the MR-fasted input model that used a sum of three IG functions, the correlation between f_1 and f_2 (0.148) was estimated as they were assigned a multivariate distribution. Since the input function was specific to each period of Study A2167, interoccasion variability was assessed only on the disposition parameters, but the variance estimates were not statistically significantly different from zero. The absorption parameters

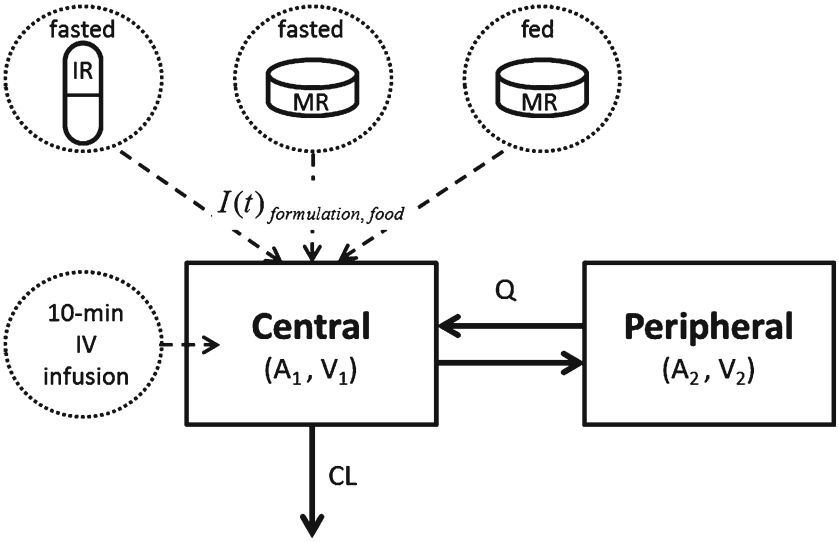

Fig. 1 Schematic representation of the final structural model for mavoglurant pharmacokinetics. *I*(*t*) (Eq. 1) is specific to the formulation and food state, and is a sum of either two or three IG density functions.

were the most variable between individuals, particularly under the MR-fed conditions. An additive error to the logarithmically-transformed plasma concentrations described adequately the unexplained residual variability. The residual error model proposed by Beal, which includes an additional random-effect compared to the additive model (24), did not improve goodness-of-fit plots of the residuals.

The demographic variable age was not tested as a covariate in the model since no marked trend was observed in the plot of the disposition parameters' empirical Bayes estimates *versus* individuals' age. Inclusion of BW as a covariate for Vc and Vp was retained in the model at the 0.0005 significance level. The relationship between BW and Vc was expressed as

$$Vc_i = \theta_{Vc}\left(\frac{BW_i}{BW_{med}}\right)^{\theta_{BW,Vc}} \times e^{(\eta_{Vc,i})} \quad (9)$$

where Vc_i is the Vc of individual i, θ_{Vc} is the standard value of Vc in the population, BW_i is the BW of individual i, BW_{med} is the population median BW, $\theta_{BW,Vc}$ is the exponent of normalised BW on Vc, and $\eta_{Vc,i}$ is the ISV in Vc for the i^{th} individual (normally distributed around zero with variance ω^2_{Vc}). The effect of BW on Vp was similarly modelled. In the studied population, lean bodyweight, fat bodyweight and predicted normal weight were not better weight descriptors for mavoglurant than BW.

The mean and standard deviation (estimate of standard error) of the bootstrap estimates are presented in Table III for the disposition parameters and in Table IV for the input parameters. Plots of the observations, individual predictions and population predictions *versus* time for three representative individuals (Fig. 2), confirm that the input functions allowed complex concentration-time profiles following oral administration of mavoglurant to be captured under all conditions (IR-fasted, MR-fasted and MR-fed), even though the absorption pattern was erratic within each sub-population (all individual goodness-of-fit plots are provided

Table III Final Estimates of Mavoglurant Disposition Parameters

Parameter	Mean[a]	% RSE[a,b]
CL (l/h)	29.3	2.48
Vc (l)	58.7	3.75
Q (l/h)	24.8	3.72
Vp (l)	113	4.48
$\theta_{BW,Vc}$	0.543	26.1
$\theta_{BW,Vp}$	1.13	12.1
ISV (% CV)[c]		
η_{CL}	32.0	11.3
η_{Vc}	28.1	16.5
η_{Q}	45.6	17.5
η_{Vp}	43.9	14.3
Covariance (correlation)		
$\eta_{CL} \sim \eta_{Vc}$	0.652	15.9
$\eta_{Q} \sim \eta_{Vp}$	0.845	17.5
Residual variability (% CV)[d]		
ε	18.3	5.87

Assessed by nonparametric bootstrapping ($n = 200$)

[a] The bootstrap estimates of the fixed-effects were back-transformed into the log-normal domain prior to calculation of the mean and standard deviation

[b] RSE: relative standard error of the estimates

[c] Calculated as $100.\sqrt{[\exp(\omega^2)-1]}$

[d] Calculated as $100.\sqrt{[\exp(\sigma^2)-1]}$

Table IV Final Estimates of Mavoglurant Input Parameters

Parameter	IR-fasted		MR-fasted		MR-fed	
	Mean[a]	% RSE[a,b]	Mean[a]	% RSE[a,b]	Mean[a]	% RSE[a,b]
F	0.436	7.09	0.387	7.57	0.508	7.55
f_1	0.591	7.89	0.199	28.4	0.0867	0.384
f_2	–	–	0.522	12.8	–	–
$tmax_1$ (h)	0.414	5.90	0.700	10.8	1.48	13.6
$tmax_2$ (h)	2.18	7.15	3.06	11.5	3.61	11.1
$tmax_3$ (h)	–	–	16.2	17.4	–	–
CV_1	0.404	0.331	1.05	27.2	1.09	18.4
CV_2	0.395	0.656	0.460	14.5	0.236	11.0
CV_3	–	–	0.422	17.4	–	–
ISV (% CV)						
η_F[c]	23.4	35.7	12.0	79.0	13.5	50.5
η_{f1}[c]	38.8	19.1	75.5	41.4	0.911 (fixed)	–
η_{f2}[c]	–	–	41.1	49.9	–	–
η_{tmax1}[d]	29.9	19.5	31.0	40.4	61.0	27.7
η_{tmax2}[d]	29.9	19.5	31.0	40.4	61.0	27.7
η_{tmax3}[d]	–	–	31.0	40.4	–	–
η_{CV1}[d]	1 (fixed)	–	38.4	38.7	53.6	19.4
η_{CV2}[d]	1 (fixed)	–	38.4	38.7	53.6	19.4
η_{CV3}[d]	–	–	38.4	38.7	–	–
Covariance (correlation)						
$\eta_{f1} \sim \eta_{f2}$	–	–	0.148	186	–	–

Assessed by nonparametric bootstrapping ($n = 200$)

[a] The bootstrap estimates of the fixed-effects were back-transformed into the log-, logit- or logistic-normal domain prior to calculation of the mean and standard deviation

[b] RSE: relative standard error of the estimates

[c] Calculated as follows: 10,000 samples were drawn from a normal distribution using the mean of the bootstrap estimates of both transformed fixed-effects and random-effects; each value was then transformed back into the logit- or logistic-normal domain, and the mean and standard deviation were computed

[d] Calculated as $100.\sqrt{[\exp(\omega^2)-1]}$ since these parameters were assumed log-normally distributed

for each formulation-food condition in the Supplementary Material online). A visual predictive check of the final model, stratified by study and by dose (Study A2121) or treatment (Study A2167), shows that the population pharmacokinetic model developed throughout the analysis adequately describes mavoglurant pooled data (Fig. 3). The lower panels indicate that the fractions of predicted BQL data reasonably accounted for the fractions of BQL data observed across time. Figure 4 demonstrates the performance of the pharmacokinetic model in predicting plasma concentration-time profiles following a single 100-mg dose of the MR tablet of mavoglurant given under fasted conditions.

Figure 5 illustrates the effect of the formulation and food conditions prior to administration, on the time course of drug input rate and fraction of bioavailable-drug provided by a single dose of 100 mg of mavoglurant. The impact of the absorption pattern on both the systemic trend and variability in the concentration-time curves provided by a twice-daily repeated administration (100 mg/dose), is depicted in Fig. 6.

DISCUSSION

In this article, we present the first model-based analysis of mavoglurant pharmacokinetics in a healthy population. Overall, its population pharmacokinetics in the studied subjects were highly variable. Elimination from the body, which is thought to be primarily mediated by hepatic metabolism (12), was linear within the studied dose range. For a standard 70 kg individual, point estimates of CL, Vc, Q and Vp were 29.3 l/h, 58.7 l, 24.8 l/h and 113 l, respectively. Considering the blood-to-plasma ratio (0.61), the blood clearance for a standard individual would be 48.0 l/h, which corresponds to approximately 55% of the hepatic blood flow (≈87.0 l/h). The variability in the disposition process was moderate and partially explained by the effect of BW on Vc and Vp, with the highest impact on Vp. This was expected for a lipophilic compound which is extensively distributed in tissues and organs once it reached the blood stream (12). No effect of BW was identified on CL. Therefore, subjects' weight is not likely

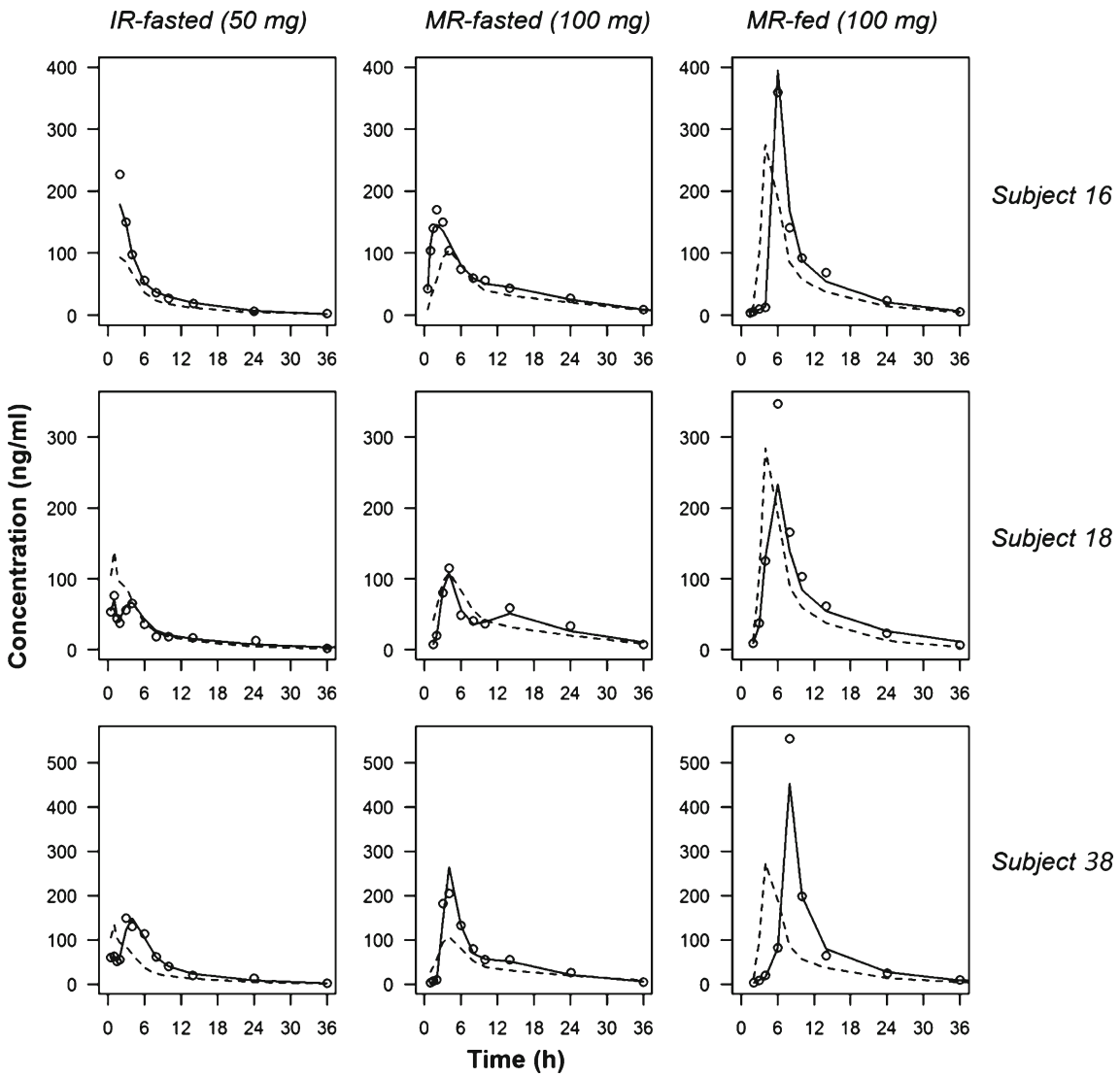

Fig. 2 Plots of the observations (*open circles*), individual predictions (*solid lines*) and population predictions (*dashed lines*) from the final mavoglurant pharmacokinetic model. Three subjects were selected to illustrate goodness-of-fit for the three formulation-food conditions (IR-fasted, MR-fasted and MR-fed).

to affect the systemic exposure to mavoglurant. No biological explanation for the correlations between CL and Vc, and between Q and Vp could be proposed since BW didn't appear to be the source of these correlations. The frequencies of female subjects and of other races than Caucasian were too low to investigate effectively the potential influence of gender and race on mavoglurant disposition. The age range of the studied subjects might also have been too narrow to evaluate the effect of age on the disposition properties.

The absorption and systemic bioavailability of an orally administered compound is governed by a number of factors that includes drug solubility, permeability, *in vivo* dissolution- or release-rate, and intestinal loss, which in turn depend on physiological, drug-, and formulation-specific factors (32). In particular, the absorption of a poorly soluble and highly permeable compound such as mavoglurant, is likely to be limited by its solubility or dissolution-rate *in vivo*, depending on the type of formulation used for oral administration. Several formulations have been clinically investigated throughout mavoglurant development. The IR capsule and the MR tablet were the two main formulations assessed in Phase I studies. The MR dosage form was developed subsequently to the IR formulation to improve drug tolerance, and has been selected for Phase II trials. To gain insight into its optimal use in patients, the input characteristics (rate and bioavailability) of the IR and MR formulations were compared in this analysis. Since the slow input process following administration of the MR formulation partly masked mavoglurant disposition, including IV data in the analysis was essential to separate the drug absorption phase from the distribution and elimination phases. Mavoglurant absorption into the systemic circulation was highly variable and difficult to describe accurately

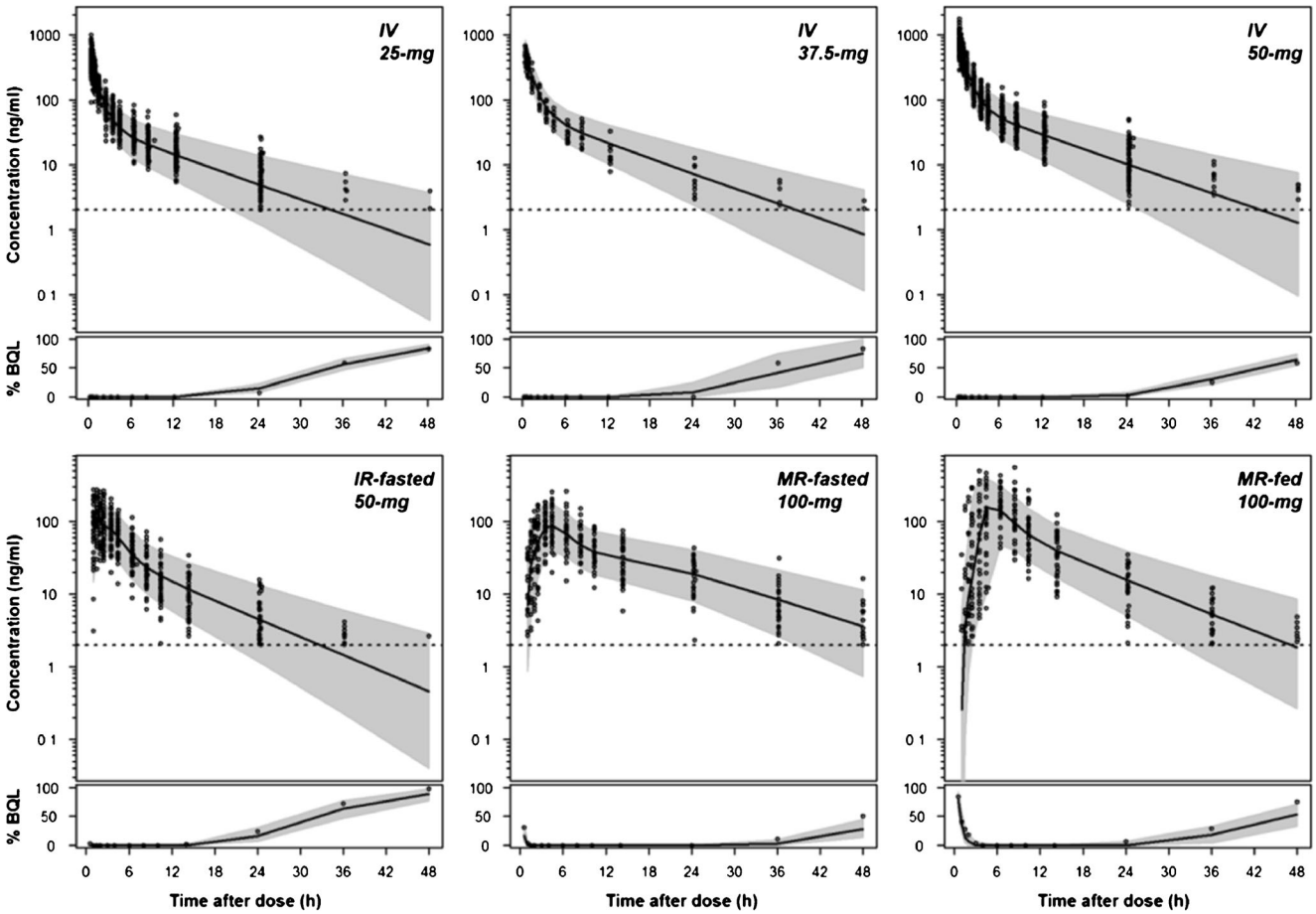

Fig. 3 Internal validation: a visual predictive check (stratified by study and dose/treatment) of the final population pharmacokinetic model's ability to predict pooled mavoglurant plasma concentration-time data from Study A2121 and Study A2167. In the *upper panels*, *open circles* represent the observed data, *solid lines* are the medians of the simulated concentrations, and the *grey shaded areas* represent a 90% prediction interval. The *horizontal dotted lines* are the limit of quantification of the assays. The *lower panels* show simulation-based 95% confidence intervals (*grey shaded areas*) around the median (*solid lines*) of the fractions of simulated BQL data (expressed in percentage). The fractions of observed BQL data are the *open circles*.

regardless of the formulation and food conditions. Although capturing adequately the complex pharmacokinetic profiles is not considered critical for prediction of drug efficacy, it is more important to predict accurately steady-state peak concentrations and anticipate drug tolerance. Using a sum of IG functions as an input rate function was deemed to be the most adequate empirical approach to capture the atypical input profiles observed in all data from Study A2167. The IG density has been previously used as a flexible function to describe the input transit time density for various drugs and extravascular administration routes (26,33–36). Summation of IG densities has been shown to offer even more flexibility to describe input processes of higher complexity such as for sustained-release products (25). Of note, a sum of log-normal density functions has been evaluated as an input rate function in this analysis and provided similar results to the sum of IG densities (results not presented). Nevertheless, the higher flexibility of the IG distribution (37) could be of greater value in other situations such as for more sustained-release formulations. An appealing aspect of such an input function is that the extent of bioavailability could be directly estimated, as it is a parameter of the function. Also, the estimated parameters can be readily used to simulate the time course of the input rate and fraction of bioavailable-drug (Eqs. (1) and (9)), and compare the input properties of different formulations or route of administration. This is of particular value during drug development for bioavailability or bioequivalence studies, and for the development of alternative routes of drug delivery. To do so in the present work, a different input rate function was estimated for each formulation and food status rather than performing a covariate analysis that would have been irrelevant given the complexity of the input model and the lack of biological meaning of the parameters.

Following administration of the IR formulation under fasted conditions, some concentration-time profiles exhibited a double-peak phenomenon, which was adequately captured by a sum of two IG functions (Fig. 1). The fact that this phenomenon was more or less pronounced across the studied

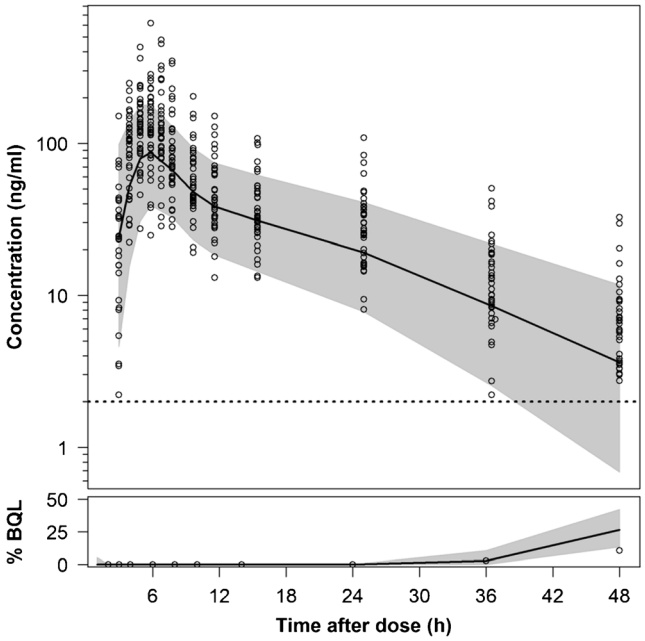

Fig. 4 External validation: a visual predictive check of the final population pharmacokinetic model's ability to predict an independent set of mavoglurant concentration-time data following administration the MR formulation under fasted conditions (Study A2171). In the *upper panel*, *open circles* represent the observed data, the *solid line* is the median of the simulated concentrations, and the *grey shaded area* represents a 90% prediction interval. The *horizontal dotted line* is the limit of quantification of the assays. The *lower panel* shows a simulation-based 95% confidence interval (*grey shaded area*) around the median (*solid line*) of the fraction of simulated BQL data (expressed in percentage). The fraction of observed BQL data is represented by the *open circles*.

subjects explains the high ISV estimated in the input parameters. The derived input function indicates that typically, there was an initial rapid entry of mavoglurant into the blood stream (maximal rate of 29.0 mg/h reached at 0.4 h) followed by a second phase of slower drug input (Fig. 5a). In addition, simulation of the time course of the fraction of bioavailable-dose suggests that the input process was typically complete within 6 h of administration of the IR capsule (Fig. 5b). Since mavoglurant is highly permeable and is *a priori* not a substrate of any transporters, absorption into the systemic circulation is thought to be limited by drug dissolution which seems to have a more complex and more variable pattern *in vivo* than *in vitro* (IR capsule designed to release the drug within approximately an hour of administration). The dissolution of the dosage form is in turn likely limited by the poor solubility of mavoglurant in aqueous media (0.025 mg/ml and pH independent). Any change in the solubility conditions along the gastrointestinal tract would thus explain the multiple-peak phenomenon. For instance, if at a given time and region of the gastrointestinal tract the volume of fluid in which the drug can be dissolved is saturated, part of the drug would remain undissolved or could precipitate until more intestinal fluid is available downstream; hence the dissolution rate would vary and the drug would appear in the circulation in a complex manner. Additional healthy volunteers' data from a single-ascending dose study of a slightly different IR formulation have shown that both the frequency and magnitude of the double-peak phenomenon was increased with increasing doses, which supports the assumption of a dissolution-limited absorption (internal unpublished data). Since mavoglurant is extensively metabolised in the liver and is substrate of the cytochrome P450 3A4 (abundant in the proximal small intestine's enterocytes), the absolute bioavailability from the IR capsule (typically 0.436 in the population) is thought to imply a significant first-pass effect due to both gut wall and hepatic metabolism.

Following administration of the MR formulation under fasted conditions, a sum of three IG functions was required to reasonably describe the complex absorption pattern characterised by a second smooth rise in plasma concentration

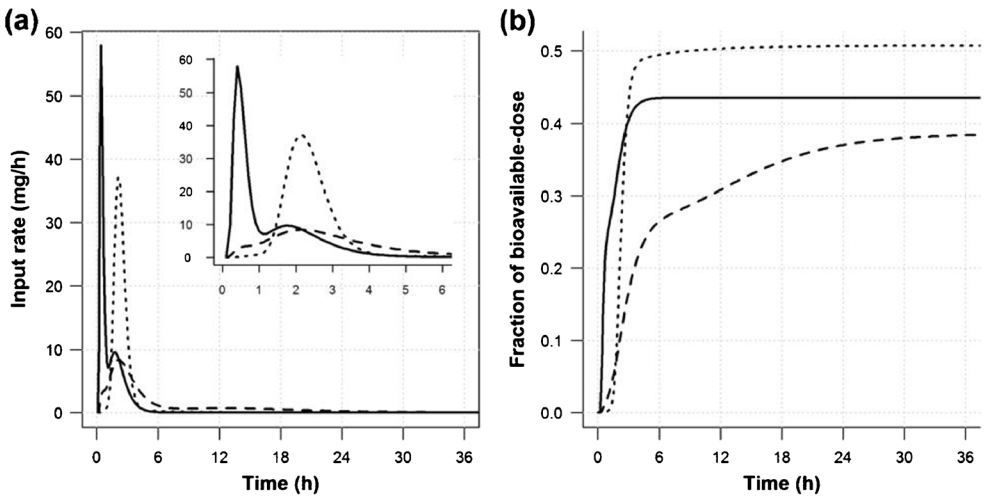

Fig. 5 Simulated standard time course of mavoglurant input rate (**a**) and fraction of bioavailable-dose (**b**) (using Eqs. (1) and (9), respectively) following a single 100-mg dose under each formulation-food condition of Study A2167, *i.e.* IR-fasted (*solid lines*), MR-fasted (*dashed lines*) and MR-fed (*dotted lines*). The insert in plot (**a**) expands the first 6 h.

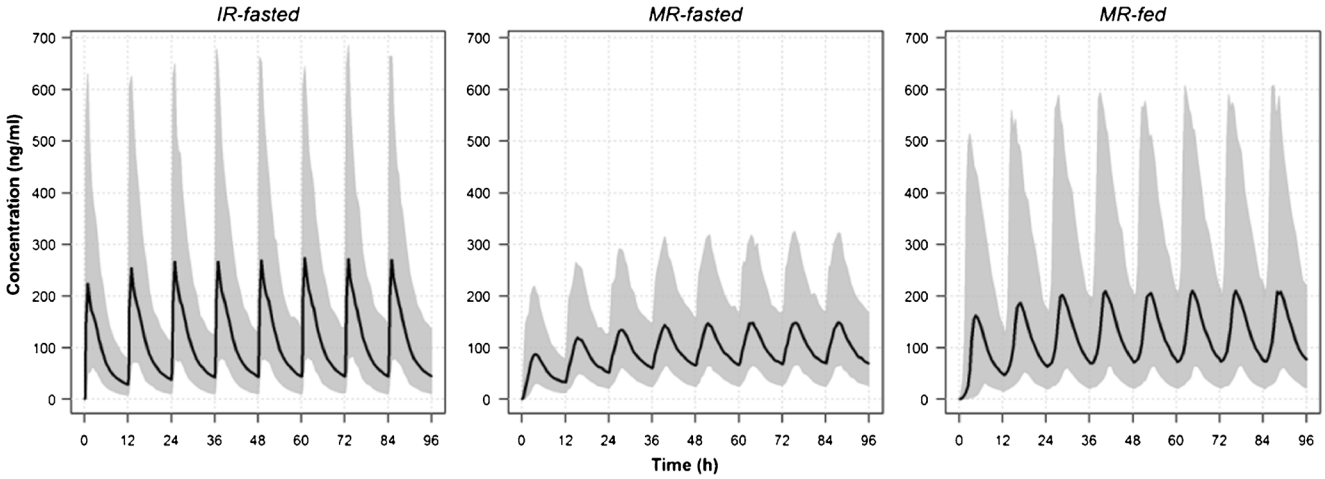

Fig. 6 Monte Carlo simulations ($n = 1000$) of mavoglurant plasma concentration-time profiles provided by a twice-daily repeated administration (100 mg/dose) of the IR formulation under fasted conditions, and of the MR formulation under both fasted and fed conditions. For each formulation-food condition, the median of the simulated concentrations (*solid line*) was plotted across time together with a 95% prediction interval (*grey shaded area*).

from approximately 8 h post dose (Fig. 2). Similarly to the IR form, this phenomenon was more or less pronounced within the studied population; hence estimates of ISV in the input parameters were high. The derived input function suggests that, at equal doses, the prolonged release of mavoglurant along the gastrointestinal tract logically resulted in a decreased rate of absorption compared to the IR formulation (maximal input rate of 8.34 mg/h reached around 2 h) which indicates that drug dissolution was the likely rate-limiting step of the input process. As for the IR form, mavoglurant absorption was typically characterised by a second phase of slower drug input (peaking at approximately 12 h) after administration of the MR tablet under fasted conditions (Fig. 5a), which was however maintained at a low rate over approximately 36 h (Fig. 5b). Although no clear physiological explanation for this pattern could be proposed given the empirical nature of the model, similar assumptions to those proposed for the IR formulation can be made for the MR formulation: any change in the dissolution conditions would yield fluctuation in the rate of drug input into the blood stream. The bioavailability from the MR tablet (0.387 for a standard individual) was lower than from the IR capsule. The long duration of the input process (≈36 h) suggests that part of the administered dose was possibly absorbed in the colon during the second phase. The colonic environment is usually less favorable for drug absorption than the small intestine (38,39). Hence, the extent of absorption might have been reduced for the MR formulation relative to the IR formulation.

When the MR tablet was administered shortly after a high fat meal, there was typically an initial delay of approximately 1 h before mavoglurant appeared in the systemic circulation (Fig. 5a). This phenomenon was highly irregular across the studied subjects and was thus reflected by the high ISV estimated for the MR-fed input function (sum of two IG functions). This initial phase of slow input is thought to be due to an erratically delayed gastric emptying of the MR tablet when administered concomitantly with food (40). Subsequently, mavoglurant was more rapidly absorbed into the blood stream than in the fasted state (maximum rate of 37.1 mg/h reached at approximately 2 h) and the late second phase of drug input was not observed. The simulated bioavailability-*versus*-time curve suggests that the input process can be considered complete 12 h post dose (Fig. 5b). Given the input properties of the MR formulation under fasted conditions, this might be explained by the increased solubility of mavoglurant by the postprandial bile salts secreted in the duodenum, thereby accelerating drug dissolution from the MR tablet. This would in turn explain the higher extent of bioavailability under fed conditions (typically 0.508 in the studied population), as well as the absence of second input phase, since most of the drug would be dissolved and be available for absorption in the small intestine.

Monte Carlo simulation ($n = 1000$) of the concentration-time profiles produced by the repeated twice-daily administration of mavoglurant IR and MR formulations under fasted and fed (for the MR formulation only) conditions, was performed to gain an understanding of the impact of the formulation- and food-specific input characteristics on the plasma concentration range at steady-state (Fig. 6). Based on visual assessment of the profiles, steady state plasma concentrations should be attained after 48 h of dosing under all formulation-food conditions, although it might be reached earlier under the IR-fasted and MR-fed conditions. Assuming that the pharmacokinetics of mavoglurant are not altered during multiple dosing, the MR formulation is expected to produce a slightly lower concentration range with lower peaks than an equivalent dose of IR capsules. This may be useful information allowing the clinician to adjust dosage of the MR tablet, in order to balance efficacy and safety during dose titration. However, the simulations also suggest a significant

food effect on the pharmacokinetic behaviour of the MR formulation: both the median trend and variability in mavoglurant steady-state plasma concentrations were increased in the fed state compared to the fasted state. As a consequence, the *a priori* reduced frequency of adverse events in patients chronically treated by mavoglurant MR formulation relative to treatment by the IR formulation, is likely dependent on the food conditions at each drug administration. Nevertheless, the standard Food and Drug Administration high-fat and high-calorie meal used in Study A2167 is not representative of the target patients' diet, which is more likely to consist of low- and medium-fat meals. Since the food effect is likely explained by the increased solubility of mavoglurant due to elevated bile salts concentrations in the duodenum, it is thought to be correlated to the meals' proportion of fat. Therefore, a less pronounced impact of the food diet on mavoglurant bioavailability and input kinetics is expected in the patient populations.

The visual predictive check (Fig. 3) indicated that the model performs well and predicts both the central trend and variability in the plasma concentration-time profiles for each route of administration, dose, formulation and food conditions. Also, discarding BQL data during the analysis didn't lead to obvious model misspecification, as indicated by the adequacy of the observed and predicted fraction of BQL data across time. A significant underprediction of the fraction of BQL data would result in bias in both input and disposition parameters. The cross-validation (Fig. 4) indicates that the model slightly underpredicted the systemic trend in Study A2171 concentration-time data for which the same MR formulation as in Study A2167 was used and healthy volunteers with similar demographics were enrolled. This might be due to the increased frequency and magnitude of the late second phase of drug input in Study A2171 data in comparison with Study A2167 data, which implies that the input function (both fixed and random effects) that would characterise Study A2171 data would be slightly different. This means that Study A2167 subjects were not very representative of the population and emphasises the high specificity of this empirical model to the data included in the analysis. In such situation, even interpolation to a similar population and similar experimental conditions is difficult. Extrapolation beyond the data, such as under different physiological conditions or for other types of formulation, would be even more challenging. Conversely, a physiologically-based model integrating prior information on drug- and formulation-specific characteristics (*e.g. in vitro* dissolution, *in vitro* metabolism and *in vitro* solubility data) would be of greater value for quantitative predictions under different conditions.

CONCLUSIONS

In summary, the disposition of mavoglurant from the body was best described by a two-compartment pharmacokinetic model, and is likely to be influenced by subjects' BW. Unlike conventional absorption models, using a sum of two or three IG functions as an input rate function described drug absorption into the systemic circulation adequately. Using the IR and MR formulations, mavoglurant input process is thought to be limited by drug dissolution which appeared to be sensitive to the physiological conditions. Even when administered in the IR formulation, mavoglurant exhibited complex and variable input characteristics. The MR formulation showed a prolonged input into the blood stream over more than a day, whereas drug input was typically complete in 6 h for the IR formulation. The bioavailability of the MR formulation was lower than for the IR form, which may be a result of the colonic absorption of part of the administered dose. Hence, dose adjustment might be required to provide a similar efficacy to the IR formulation. A repeated twice-daily administration of the MR tablet is expected to produce smaller peak-to-trough variation than the IR formulation, which might allow a reduction of the frequency of side effects reported in the clinical studies that used the IR form. The input properties of the MR tablet appeared to be strongly governed by the food conditions at drug administration, although the standard high fat meal used to assess food effect on drug input represents an extreme case scenario and is probably not representative of the target patient populations' diet.

ACKNOWLEDGMENTS AND DISCLOSURES

The authors thank Nikolaos Tsamandouras (Manchester Pharmacy School, The University of Manchester, Manchester, United-Kingdom), for providing technical support including the methodology on the use of the logistic-normal distribution; Andres Olivares-Morales (Manchester Pharmacy School, The University of Manchester, Manchester, United-Kingdom) for the invaluable discussions on absorption mechanisms; Subramanian Ganesan (Drug Metabolism and Pharmacokinetics, Novartis Institutes for Biomedical Research, Hyderabad, India) for the useful discussions on mavoglurant pharmacokinetics.

REFERENCES

1. Glass IA. X linked mental retardation. J Med Genet. 1991;28:361–71.
2. Brown WT, Jenkins EC, Cohen IL, Fisch GS, Wolf-Schein EG, Gross A, *et al.* Fragile X and autism: a multicenter survey. Am J Med Genet. 1986;23:341–52.
3. Li SY, Chen YC, Lai TJ, Hsu CY, Wang YC. Molecular and cytogenetic analyses of autism in Taiwan. Hum Genet. 1993;92:441–5.
4. Estecio M, Fett-Conte AC, Varella-Garcia M, Fridman C, Silva AE. Molecular and cytogenetic analyses on Brazilian youths with pervasive developmental disorders. J Autism Dev Disord. 2002;32:35–41.

5. Reddy KS. Cytogenetic abnormalities and fragile-X syndrome in autism spectrum disorder. BMC Med Genet. 2005;6:3.
6. Bagni C, Tassone F, Neri G, Hagerman R. Fragile X syndrome: causes, diagnosis, mechanisms, and therapeutics. J Clin Invest. 2012;122:4314–22.
7. Dolen G, Carpenter RL, Ocain TD, Bear MF. Mechanism-based approaches to treating fragile X. Pharmacol Ther. 2010;127:78–93.
8. Levenga J, Hayashi S, de Vrij FM, Koekkoek SK, van der Linde HC, Nieuwenhuizen I, *et al.* AFQ056, a new mGluR5 antagonist for treatment of fragile X syndrome. Neurobiol Dis. 2011;42:311–7.
9. Gantois I, Pop AS, de Esch CE, Buijsen RA, Pooters T, Gomez-Mancilla B, *et al.* Chronic administration of AFQ056/Mavoglurant restores social behaviour in Fmr1 knockout mice. Behav Brain Res. 2013;239:72–9.
10. Pop AS, Levenga J, de Esch CE, Buijsen RA, Nieuwenhuizen IM, Li T, *et al.* Rescue of dendritic spine phenotype in Fmr1 KO mice with the mGluR5 antagonist AFQ056/Mavoglurant. Psychopharmacology. 2014;231:1227–35.
11. Jacquemont S, Curie A, des Portes V, Torrioli MG, Berry-Kravis E, Hagerman RJ, *et al.* Epigenetic modification of the FMR1 gene in fragile X syndrome is associated with differential response to the mGluR5 antagonist AFQ056. Sci Transl Med. 2011;3:64ra61.
12. Walles M, Wolf T, Jin Y, Ritzau M, Leuthold LA, Krauser J, *et al.* Metabolism and disposition of the metabotropic glutamate receptor 5 antagonist (mGluR5) mavoglurant (AFQ056) in healthy subjects. Drug Metab Dispos. 2013;41:1626–41.
13. Berg D, Godau J, Trenkwalder C, Eggert K, Csoti I, Storch A, *et al.* AFQ056 treatment of levodopa-induced dyskinesias: results of 2 randomized controlled trials. Mov Disord. 2011;26:1243–50.
14. Stocchi F, Rascol O, Destee A, Hattori N, Hauser RA, Lang AE, *et al.* AFQ056 in Parkinson patients with levodopa-induced dyskinesia: 13-week, randomized, dose-finding study. Mov Disord. 2013;28:1838–46.
15. Custodio JM, Wu CY, Benet LZ. Predicting drug disposition, absorption/elimination/transporter interplay and the role of food on drug absorption. Adv Drug Deliv Rev. 2008;60:717–33.
16. Zhou H. Pharmacokinetic strategies in deciphering atypical drug absorption profiles. J Clin Pharmacol. 2003;43:211–27.
17. Jakab A, Winter S, Raccuglia M, Picard F, Dumitras S, Woessner R, *et al.* Validation of an LC-MS/MS method for the quantitative determination of mavoglurant (AFQ056) in human plasma. Anal Bioanal Chem. 2013;405:215–23.
18. Beal SL, Sheiner LB, Boeckmann AJ, Bauer RJ. NONMEM 7.2.0 users' guides. Ellicott City: ICON Development Solutions; 2011.
19. Lindbom L, Pihlgren P, Jonsson EN. PsN-Toolkit–a collection of computer intensive statistical methods for non-linear mixed effect modeling using NONMEM. Comput Methods Prog Biomed. 2005;79:241–57.
20. R.D.C. Team. R: a language and environment for statistical computing. Vienna: R Foundation for Statistical Computing; 2009.
21. Savic RM, Jonker DM, Kerbusch T, Karlsson MO. Implementation of a transit compartment model for describing drug absorption in pharmacokinetic studies. J Pharmacokinet Pharmacodyn. 2007;34:711–26.
22. Holford NH, Ambros RJ, Stoeckel K. Models for describing absorption rate and estimating extent of bioavailability: application to cefetamet pivoxil. J Pharmacokinet Biopharm. 1992;20:421–42.
23. Karlsson MO, Sheiner LB. The importance of modeling interoccasion variability in population pharmacokinetic analyses. J Pharmacokinet Biopharm. 1993;21:735–50.
24. Beal SL. Ways to fit a PK model with some data below the quantification limit. J Pharmacokinet Pharmacodyn. 2001;28:481–504.
25. Csajka C, Drover D, Verotta D. The use of a sum of inverse Gaussian functions to describe the absorption profile of drugs exhibiting complex absorption. Pharm Res. 2005;22:1227–35.
26. Weiss M. A novel extravascular input function for the assessment of drug absorption in bioavailability studies. Pharm Res. 1996;13:1547–53.
27. Gueorguieva I, Ogungbenro K, Graham G, Glatt S, Aarons L. A program for individual and population optimal design for univariate and multivariate response pharmacokinetic-pharmacodynamic models. Comput Methods Prog Biomed. 2007;86:51–61.
28. Duffull SB, Dooley MJ, Green B, Poole SG, Kirkpatrick CM. A standard weight descriptor for dose adjustment in the obese patient. Clin Pharmacokinet. 2004;43:1167–78.
29. Savic RM, Karlsson MO. Importance of shrinkage in empirical bayes estimates for diagnostics: problems and solutions. AAPS J. 2009;11:558–69.
30. Bergstrand M, Karlsson MO. Handling data below the limit of quantification in mixed effect models. AAPS J. 2009;11:371–80.
31. Shen J, Boeckmann A, Vick A. Implementation of dose superimposition to introduce multiple doses for a mathematical absorption model (transit compartment model). J Pharmacokinet Pharmacodyn. 2012;39:251–62.
32. Martinez MN, Amidon GL. A mechanistic approach to understanding the factors affecting drug absorption: a review of fundamentals. J Clin Pharmacol. 2002;42:620–43.
33. Karmakar MK, Ho AM, Law BK, Wong AS, Shafer SL, Gin T. Arterial and venous pharmacokinetics of ropivacaine with and without epinephrine after thoracic paravertebral block. Anesthesiology. 2005;103:704–11.
34. Kirchheiner J, Brockmoller J, Meineke I, Bauer S, Rohde W, Meisel C, *et al.* Impact of CYP2C9 amino acid polymorphisms on glyburide kinetics and on the insulin and glucose response in healthy volunteers. Clin Pharmacol Ther. 2002;71:286–96.
35. Lotsch J, Weiss M, Ahne G, Kobal G, Geisslinger G. Pharmacokinetic modeling of M6G formation after oral administration of morphine in healthy volunteers. Anesthesiology. 1999;90:1026–38.
36. Zhang X, Nieforth K, Lang JM, Rouzier-Panis R, Reynes J, Dorr A, *et al.* Pharmacokinetics of plasma enfuvirtide after subcutaneous administration to patients with human immunodeficiency virus: Inverse Gaussian density absorption and 2-compartment disposition. Clin Pharmacol Ther. 2002;72:10–9.
37. Chhikara R, Folks JL. The inverse Gaussian distribution as a lifetime model. Technometrics. 1977;19:461–8.
38. Tannergren C, Bergendal A, Lennernas H, Abrahamsson B. Toward an increased understanding of the barriers to colonic drug absorption in humans: implications for early controlled release candidate assessment. Mol Pharm. 2009;6:60–73.
39. Olivares-Morales A, Kamiyama Y, Darwich A, Aarons L, Rostami-Hodjegan A. Analysis of the impact of controlled release formulations on oral drug absorption, gut wall metabolism and relative bioavailability of CYP3A substrates using a physiologically-based pharmacokinetic model. Eur J Pharm Sci. 2014. doi:10.1016/j.ejps.2014.10.018.
40. Weitschies W, Wedemeyer RS, Kosch O, Fach K, Nagel S, Soderlind E, *et al.* Impact of the intragastric location of extended release tablets on food interactions. J Control Release Off J Control Release Soc. 2005;108:375–85.